Research article

Innate Immunity

17(3) (2011) 327–337

ISSN 1753-4259 (print)
10.1177/1753425910370709

# Contribution of the C-terminal end of apolipoprotein AI to neutralization of lipopolysaccharide endotoxic effect

María F. Henning[1], Vanesa Herlax[1], Laura Bakás[1,2]

[1]*Instituto de Investigaciones Bioquímicas La Plata (INIBIOLP), CCT La Plata, CONICET, Facultad de Ciencias Médicas, UNLP, La Plata, Argentina*
[2]*Departamento de Ciencias Biológicas, Facultad de Ciencias Exactas, Universidad Nacional de La Plata, La Plata, Argentina*

It is well known that high density lipoprotein (HDL) binds bacterial lipopolysaccharide (LPS) and neutralizes its toxicity. The aim of this work was to study changes in the apolipoprotein (apo) AI structure after its interaction with LPS as well as to determine the protein domain involved in that interaction. The presented data indicate that LPS does not lead to major changes in the structure of apoAI, judging from Trp fluorescence spectra. However, analysis of denaturation behavior and binding of ANS show that LPS induces a loosened protein conformation. Further evidence for an apoAI–LPS specific interaction was obtained by incubation of the protein with $^{125}$I-ASD-LPS. The results show that multiple regions of the protein were able to interact with LPS, according to its amphiphatic nature. Finally, the contribution of the purified C-terminal fragment of the protein in the endotoxin neutralization was evaluated in comparison with the effect of apoAI. In both cases, the same decrease in tumor necrosis factor-α released was observed. This result suggests that the C-terminal half of apoAI is the main domain responsible of the neutralization effect of this protein. Our data may provide innovative pharmacological tools in endotoxin neutralization therapies.

*Keywords:* lipoprotein, TNF-alpha, ASD-LPS, ANS, GdnHCl denaturation

*Abbreviations:* apolipoprotein (apo) AI, apoAI; LPS, lipopolysaccharide; SASD, sulfosuccinimidyl 2-(-azidosalicylamido)-1,3′-dithiopropionate; ASD, 2-(*p*-azidosalicylamido)-1,3′-dithiopropionate; ASD-LPS, ASD-coupled LPS; $^{125}$I-ASD-LPS, $^{125}$I-iodinated ASD-LPS; PAGE, polyacrylamide gel electrophoresis; PBS, phosphate-buffered saline (pH 7.2); SDS, sodium dodecyl sulfate. ANS, 1-anilino-naphthalene-1,3,5-sulfonate; rHDL, reconstituted high density lipoprotein; LUV, large unilamellar vesicle; NBS, *N*-bromosuccinimide; POPC, 1-palmitoyl-2-oleyl phosphatidylcholine; Trp, tryptophan; CD, circular dichroism; TNF-α, tumor necrosis factor-α

## Introduction

Lipopolysaccharide (LPS), the toxic component present in the outer membrane of Gram-negative bacteria, is the major pathogenic factor in sepsis. When LPS enters the blood-stream, it elicits inflammatory responses that may lead to septic shock and, ultimately, death.

Wu *et al.*[1] reported that high-density lipoproteins (HDL) might possess anti-inflammatory properties and play a crucial role in innate immunity by regulating the inflammatory response as well as reducing the severity of organ injury in animals and patients with septic shock via LPS-binding and neutralization.

However, HDL has been shown to be substantially reduced as part of an acute-phase response to infections and the magnitude of this reduction is positively correlated with the severity of illness.[2,3] In the acute-phase response, plasma HDL changes from anti-inflammatory

Received 2 February 2010; Revised 18 March 2010; Accepted 30 March 2010

Correspondence to: Dr Laura Bakás, INIBIOLP-Facultad de Ciencias Médicas. Calles 60 y 120 (1900), La Plata, Argentina.
E-mail: lbakas@biol.unlp.edu.ar

to pro-inflammatory,[4] which may render the patient more susceptible to pro-inflammatory stimuli. The mechanisms underlying this phenomenon are poorly understood, although increased levels of several acute-phase proteins, including serum amyloid A (SAA) and secretory phospholipase $A_2$ (sPLA2) may contribute to the decrease in plasma HDL.

Studies in humans demonstrated that the LPS-induced production of tumor necrosis factor (TNF)-α in blood samples, taken from critically ill patients, was reduced by the supplementation of a reconstituted HDL (rHDL) preparation.[5]

Several studies indicate that the anti-endotoxin function of HDL is due to the interaction between the lipid portion of the LPS molecule and phospholipid in HDL.[6] Previous evidence from our laboratory (Henning *et al*., unpublished results) shows that incubation of LPS with liposomes decreases the amount of TNF-α released from RAW cells. However, other authors reported that apoAI might be the major neutralizing factor,[7,8] instead of HDL lipids.

Apolipoprotein (apo) AI, the major protein component of serum HDL, has an amphipathic α-helical structure. The lipid binding sites on the amphipathic α-helix may be the domain involved in the interaction with LPS via the lipid A moiety. Thus, apoAI should be a safe and effective treatment to prevent or reverse the consequences of endotoxemia and tissue inflammatory injury.

The direct inactivation of endotoxin effect by free apoAI was demonstrated by Emancipator *et al*.[9] in *in vitro* studies. More recently, Yan *et al*.[10] observed that apoAI could: (i) attenuate LPS-induced acute lung injury and inflammation; (ii) significantly inhibit LPS-induced inflammatory cytokine levels in serum; (iii) inhibit L-929 cell death induced by LPS-activated macrophages in a dose-dependent fashion; and (iv) significantly decrease the mortality of mice with endotoxemia.

Furthermore, Ma *et al*. showed that apoAI inhibited macrophage activation when the protein was pre-incubated with LPS. Also, they observed that apoAI binds LPS indirectly by LPS binding protein (LBP), albeit it can bind LPS directly and neutralize its cytotoxicity.[11]

The molecular understanding of the LPS neutralization process by apoAI requires knowledge of the molecular conformation of lipid-free apoAI and the conformational changes that it suffers after binding to LPS.

In this context, the purpose of this study was to investigate the effects of LPS on the structure of apoAI and characterize the apoAI domain involved in this interaction. In this research, we show data about the neutralization of the endotoxic LPS effects by the C-terminal end of apoAI.

## Materials and Methods

### *Protein purification*

Apolipoprotein AI was purified from the HDL fraction of human serum (kindly donated by the Banco de Sangre del Instituto de Hemoterapia de la Provincia de Buenos Aires, La Plata, Argentina) according to the procedure previously described,[12] and stored in lyophilized form at −70°C. Before each experiment, apoAI was solubilized in 3 M guanidinium hydrochloride (GdnHCl) and dialyzed extensively against buffer A (10 mM Tris, 150 mM NaCl, 1 mM EDTA, 1 mM $NaN_3$, pH 8.0; 1 : 2000, v : v) for 18 h at 4°C.

### *Apolipoprotein AI–LPS interaction*

Lipopolysaccharide (LPS) from *Escherichia coli* O111:B4 was purchased from Sigma Aldrich (St Louis, MO, USA).

For all experiments, apoAI (2.85 μmol) was incubated with LPS (1 : 2.8, molar ratio) at 25°C for 15 min in buffer A. The molecular mass taken for LPS was of 10 kDa, according to Aurell and Winstrom.[13]

### *Fluorescence spectroscopy*

Protein intrinsic fluorescence spectra were recorded on a Perkin-Elmer LS 50B spectrofluorimeter with a temperature-controlled sample holder. The excitation wavelength used was 295 nm to minimize tyrosine emission.[14] Fluorescence was measured after incubating apoAI with LPS. Spectra were recorded in the range 320–400 nm using 150-μl cuvettes (4 nm slit width for both excitation and emission).

### *Chemical modification of apoAI with N-bromosuccinimide (NBS)*

A freshly prepared solution of NBS was added to apoAI or apoAI–LPS mixture to achieve NBS:Trp molar ratios ranging from 0.25 : 1 to 2 : 1. (mol : mol).[15] After equilibrating for 10 min, the Trp emission spectra were recorded in the wavelength range 300–400 nm. The excitation wavelength used was 295 nm and fluorescence measurements were corrected for any dilution factor.

### *Fluorescence of ANS*

Fluorescence spectra of 8-anilino-1-naphthalenesulfonic acid (ANS) were obtained in buffer A and in the presence of apoAI or apoAI–LPS. Since ANS fluorescence in buffer is negligible,[16] spectra were recorded in

an excess of ANS (100 μM) with respect to protein (mol per mol). Samples were excited at 395 nm with emission monitored from 400 to 600 nm (4 nm slit width for both excitation and emission).

### *Guanidinium hydrochloride denaturation*

Fluorescence emission of Trp was used to monitor apoAI denaturation at increasing concentrations of GdnHCl, in the absence and presence of LPS. Chemical stability was measured after incubating apoAI or apoAI–LPS at various GdnHCl concentrations (0–5.5 M), buffered with buffer A at 25°C for 2 h. After incubation, the Trp fluorescence spectra were recorded in the range 320–400 nm using 150-μl cuvettes. The fluorescence intensity at 333 nm was used to calculate $f_D$ (molar fraction of denatured molecules)[17] as follows:

$$f_D = Xx - X_{\text{GdnHCl 0 M}}/X_{\text{GdnHCl 5.5 M}} - X_{\text{GdnHCl 0 M}} \quad (1)$$

where $Xx$ is the fluorescence intensity at 333 nm at each GdnHCl concentration tested.

### *Far-UV circular dichroism spectroscopy*

Spectra were recorded on a Jasco J-810 spectropolarimeter. Data in the far-UV (190–250 nm) region were collected using a 1-mm path cuvette. The sample chamber was maintained at 25°C. A scan speed of 20 nm/min with a time constant of 1 s was used. ApoAI or apoAI–LPS (0.1 mg/ml protein concentration) were dissolved in 50 mM sodium phosphate, pH 7.0.

Each spectrum was measured at least three times, and the data were averaged to reduce noise. Molar ellipticity was calculated as described elsewhere, using mean residue weight values of 114.45 for apoAI.[18] The α-helix content of apoAI or apoAI–LPS was calculated as described by Chen *et al*.[19]

### *Synthesis of ASD–LPS*

Synthesis of 2-(*p*-azidosalicylamido)-1,3′-dithiopropionate (ASD)-LPS was done as described by Wollenweber,[20] with some modifications. Briefly, 1.5 ml of *E. coli* O111: B4 LPS (2 mg/ml) in 5 mM EDTA pH 7.4, was mixed with 1.5 ml of 0.1 M borate pH 8.5. Six milligrams of sulfosuccinimidyl 2-(*p*-azidosalicylamido)-1,3′-dithiopropionate (SASD, Pierce Chemical Co.) were added to LPS-borate and the solution was briefly sonicated (model W-375, Ultrasonics); then, the reaction mixture was kept at 20°C for 30 min. An additional incubation with 6 mg of fresh SASD was done under the described conditions. Lipopolysaccharide coupled to ASD–LPS was centrifuged to pellet remains of SASD (2000 *g* for 2 min) followed by dialysis of the cleared supernatant against 50 mM HEPES, 5 mM EDTA pH 7.4, at 4°C (minimum six changes), aliquoted (250 μl), and stored at −20°C.

All reactions with photosensitive compounds were carried out under reduced lighting using a 25-W red light source.

### *Radio-iodination of ASD–LPS*

Iodination of ASD–LPS was carried out according to Ulevitch[21] with minor modifications. Carrier-free $Na^{125}I$ (5 mCi in 14 μl of 0.1 M NaOH; NEN Perkin Elmer) was added to 250 μl of ASD–LPS in the presence of 50 μl of 0.1 mg/ml chloramine-T (Sigma) in freshly prepared 5 mM EDTA pH 7.4, and left for 5 min at 20°C. The reaction was stopped with 50 μl of 0.1 mg/ml sodium metabisulfate freshly prepared in 5 mM EDTA pH 7.4. The reaction mixture was dialyzed extensively against 50 mM HEPES, 5 mM EDTA pH 7.4, at 4°C until less than 0.5% of total radioactivity could be measured in the outer dialysate. The $^{125}$I-ASD–LPS was collected and its radioactivity checked. The LPS concentration of this sample was determined by the 3-deoxy-D-*manno*-oct-2-ulosonic acid content employing a colorimetric microassay.[22]

### *Cross-linking of apoAI-$^{125}$I-ASD–LPS*

Five microlitres of $^{125}$I-ASD–LPS containing approximately 5 μg of LPS were incubated in the presence of apoAI in borosilicate glass tubes for 1 h in a 25°C water bath. Samples subjected to photolysis were irradiated for 1 min with short-wave UV light with a Xenon lamp (450 W) at a distance of 25 cm.

Sodium dodecyl sulfate-gel electrophoresis sample buffer was added to a final concentration of 62.5 mM Tris-HC1, pH 6.8, 3% SDS, 10% glycerol, 0.02% bromophenyl blue, with or without 0.1 M dithioerythritol. Approximately equal aliquots of radioactivity were applied onto SDS-PAGE, and electrophoresis was carried out according to Laemmli[23] on 4–25% continuous gradient gels. Proteins were stained with Coomassie Blue R250 (Sigma) and destained with several washes (5–6 times) in water/methanol/acetic acid (50 : 40 : 10, v : v : v) at 20°C, including 3.5% glycerol in a final soaking. Gels were dried on a Slab Gel Dryer (Bio-Rad) and subsequent autoradiography was performed on a scanner model Storm 840.

### *Chemical cleavage of apoAI-$^{125}$I-ASD–LPS with CNBr*

For cleavage of apoAI-$^{125}$I-ASD–LPS with CNBr, protein was dissolved in 50 μl of 70% formic acid, and

CNBr was added in a 30 : 1 CNBr : protein w/w ratio and incubated at 25°C under a $N_2$ atmosphere for 24 h. Then the samples were dried in a Speed Vac system and redissolved in 20 µl of sample buffer for tricine SDS-PAGE analysis. Sodium dodecyl sulfate-PAGE was carried out according to Schägger[24] in 17% acrylamide Tris-tricine gel. After fixing with methanol : acetic (50 : 10 v : v), the gel was stained with 0.025% Coomassie Blue R250 in 10% acetic acid. Gels were dried and exposed to X-Omat film (Kodak) for different times depending on the amount of radioactivity.

### *N-Terminal sequencing of apoAI fragments*

Peptide fragments obtained by CNBr proteolysis were transferred from tricine-SDS-PAGE to polyvinylidene difluoride (PVDF) membranes using a Trans-Blot semi-dry transfer cell (Bio-Rad) at 100 V for 40 min. N-Terminal sequencing was performed on the bands in PVDF membranes using Edman method by the Laboratorio Nacional de Investigación y Sevicio en Péptidos y Proteínas (LaNaIS Pro, Universidad de Buenos Aires-Consejo Nacional de Investigaciones Científicas y Técnicas, Buenos Aires, Argentina).

### *Electroelution*

After CNBr proteolysis of apoAI, the proteolytic products were separated by electrophoresis on Tris-tricine gels and then the fragment of interest (C-terminal) was isolated from the gels by electroelution using BioRad equipment.[25,26] After electroelution, the sample was concentrated and checked by tricine SDS-PAGE. The fragment concentration was determined by the method of Lowry *et al*.[27]

### *Tumor necrosis factor-α release measurements*

With the aim to study if apoAI and C-terminal fragment neutralize the endotoxic effect of LPS, macrophages from the cell line RAW 264.7 were exposed to LPS or apoAI/C-terminal fragment : LPS mixtures and the TNF-α released was quantified. The ratios used were 1 : 1 and 1 : 10 w/w LPS to apoAI or C-terminal fragment. For cell stimulation, the cultures were incubated, with LPS or apoAI/fragment-LPS mixtures at a LPS final concentration of 10 ng/ml, for 4 h at 37°C under 5% $CO_2$. After 10-min centrifugation at 400 *g*, supernatants were collected, fractioned and stored at −20°C until their use for the immunological determination of TNF-α by a sandwich ELISA method using BD OptEIA kit. All experiments were carried out three times. Data were expressed as mean ± SE and analyzed using Student's *t*-test (Instat 2.0 Graph Pad Software, San Diego, CA, USA).

## RESULTS

### *Steady-state fluorescence spectroscopy of lipid-free apoAI and apoAI–LPS*

Apolipoprotein AI has four Trp residues located in the amino-terminal portion of the protein (residues 8, 50, 72 and 108) and their fluorescence is sensitive to the environment. We proceeded to study the fluorescence properties of apoAI in its lipid-free form and after its incubation with LPS.

The wavelength of maximum fluorescence ($\lambda_{max}$) indicates the polarity of the Trp environment. Burstein *et al*.[28] classified Trp residues depending on the maximum ranges as follows: class I (330–332 nm), buried in non-polar regions of protein; class II (340–342 nm), surface but limited solvent contact; and class III (350–352 nm), completely solvent exposed.

Concerning the lipid-free apoAI in buffer A, it exhibits a $\lambda_{max}$ of 336 nm that represents the average environment of all the Trp residues in the protein. After its incubation with LPS, $\lambda_{max}$ was red-shifted about 0.5–1 nm, indicating that Trp exists in the free form, located in a minimally solvent exposed environment. The fluorescence spectra of apoAI in the lipid-free form and its complex with LPS are shown in Figure 1.

Although no changes in the $\lambda_{max}$ of Trp spectra was observed, there is an important decrease in the intrinsic fluorescence intensity of apoAI after LPS addition.

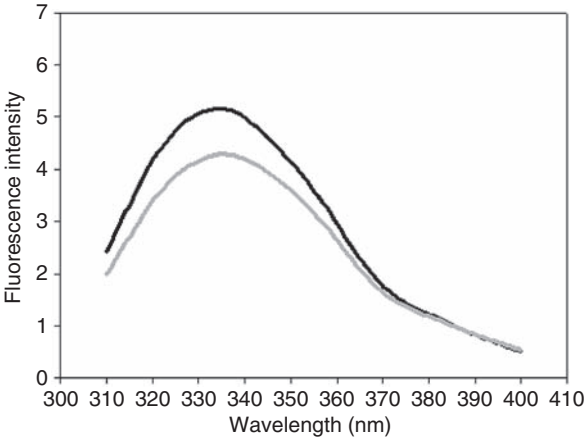


**Fig. 1**. Steady-state fluorescence spectroscopy of lipid-free apoAI (black line) and LPS-bound apoAI (gray line). The emission spectra (300–400 nm) were measured at 25°C and the excitation wavelength used was 295 nm. Protein concentration used in both cases was 2.85 µM. ApoAI–LPS (1 : 2.8 molar ratio) were previously incubated for 15 min.

*Chemical modification of Trp with N-bromosuccinimide*

To determine precisely the relative exposure of each Trp residue to LPS, apoAI was subjected to oxidation with *N*-bromosuccinimide (NBS). Experiments were performed at neutral pH to increase the specificity for Trp residues. Under these conditions, the reaction of NBS with Trp in apoAI is almost accomplished within 10 min of incubation (data not shown).

As shown in Figure 2, fluorescence decreases approximately 50% in both free and LPS-bound apoAI suggesting, that some of the Trp residues are completely protected from solvent. The $\lambda_{max}$ and NBS oxidation data show that all Trp residues are surface located but with limited solvent contact. No differences were observed in the oxidation of Trp in presence of LPS. So, the results suggest that the N-terminal half of apoAI, where the Trp residues are located, is not involved in its LPS interaction.

*8-Anilino-1-naphthalenesulfonic acid (ANS) binding experiments*

To probe changes on the molecular organization of lipid-free apoAI after its interaction with LPS further, the fluorescence properties of ANS were determined.

8-Anilino-1-naphthalenesulfonic acid is a dye whose intrinsic fluorescence increases upon binding to a hydrophobic surface or cavity.[16] In the absence of protein, ANS has a very low quantum yield with an emission wavelength maximum at 515 nm ($\lambda_{exc}$ 395 nm). The addition of apoAI induces an enhancement in ANS fluorescence quantum yield (Fig. 3A). A significantly higher fluorescence increase was observed when apoAI was previously incubated with LPS (Fig. 3B), suggesting that the relative amount of ANS-accessible hydrophobic surface in the protein is increased by LPS interaction. Controls of enhancement of ANS fluorescence due to LPS were done. Any fluorescence increase was observed, indicating that the large enhancement of ANS fluorescence may be due to the looseness of the apoAI conformation induced by LPS.

Resonance energy transfer between Trp residues and ANS molecules has been reported, so energy transfer efficiency was calculated from the decrease in donor fluorescence for both free apoAI or after incubation of apoAI with LPS (data not shown). Both results were similar supporting the idea that LPS does not interact with the N-terminal portion of apoAI, where most of the Trp residues are located.

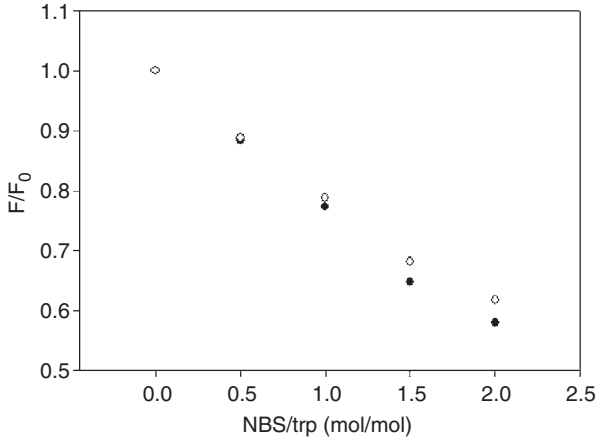


**Fig. 2**. Chemical modification of Trp with *N*-bromosuccinimide. Intrinsic fluorescence of apoAI (filled circles) or apoAI after LPS incubation (open circles) was measured after NBS addition. The Trp emission spectra were recorded in the wavelength range 300–400 nm. $F_o$ and $F$ represent the intrinsic fluorescence of native and oxidized protein, respectively. Protein concentration used in both cases was 2.85 μM. ApoAI–LPS (1 : 2.8 molar ratio) were previously incubated for 15 min.

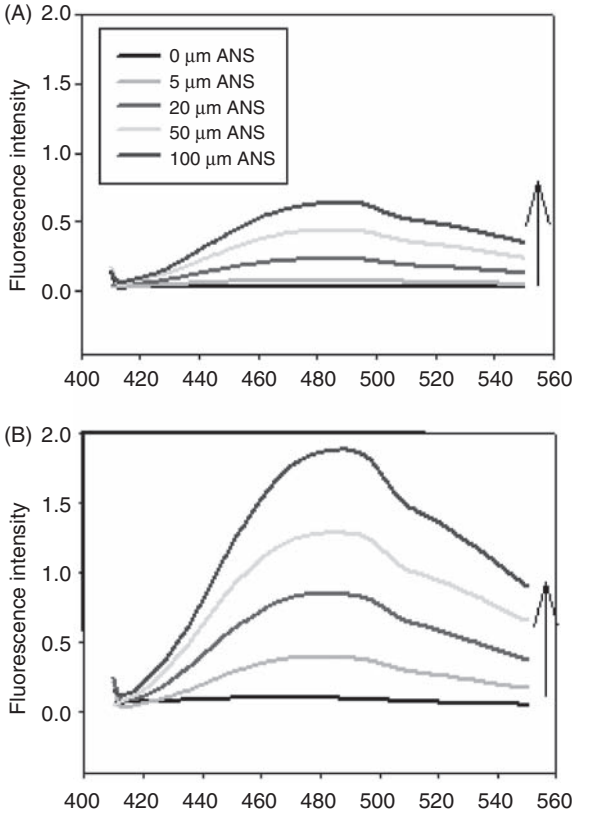


**Fig. 3**. ANS binding experiments. Fluorescence spectra of ANS were obtained in the presence of apoAI (A) or apoAI-LPS (1 : 2.8 molar ratio, previously incubated) (B). Spectra were recorded for increasing ANS concentrations (0–100 μM). Samples were excited at 295 nm with emission monitored from 400–550 nm. Protein concentration in both cases was 2.85 μM.

*Guanidinium hydrochloride denaturation*

Denaturation curves are suitable for measuring differences in conformational stability among proteins. The relative concentration of folded (native) and unfolded conformations can be determined from studies in which spectral probes such Trp, are used to monitor the conformational state of the protein.[29] The fluorescence intensity of Trp decreases upon denaturation. Employing the intensity value at 333 nm for each GdnHCl concentration tested, it was possible to estimate $f_D$ (mole fraction of denatured molecules) (Fig. 4A).

Guanidinium hydrochloride unfolding transitions reached a plateau, and a two-model state fits the experimental data. The GdnHCl concentration required to reach the mid-point of the transition between both states ($C_m$) was 1.4 for both apoAI in buffer and after its interaction with LPS. However, as seen in Figure 4A, the presence of LPS decreases the co-operativity of the unfolding process.

Because the unfolding event consists of an equilibrium process involving two states, it allows the definition of the equilibrium constant $K = f_D/(1 - f_D)$. Hence, the Gibb's free energy ($\Delta G^\circ$) for the unfolding reaction in terms of these mole fractions at a particular GdnHCl concentration ($\Delta G^\circ = -RT \ln K$) can be calculated. The dependence of $\Delta G^\circ$ on GdnHCl concentration can be approximated by the linear equation $\Delta G^\circ = \Delta G^\circ_{H_2O} - m$ [GdnHCl], where the free energy of unfolding in the absence of denaturant ($G^\circ_{H_2O}$), which represents the conformational stability of the protein, can be obtained by extrapolating to zero denaturant concentration. The coefficient $m$ is proportional to the amount of hydrophobic regions of the protein that are exposed to solvent when the protein unfolds.[30] Figure 4B shows that $\Delta G^\circ_{H_2O}$ and $m$ change in the presence of LPS. $\Delta G^\circ_{H_2O}$ decreases from 3544 cal/mol to 1426 cal/mol and $m$ also decreases from 2207 to 937 for apoAI in buffer or after its interaction with LPS, respectively.

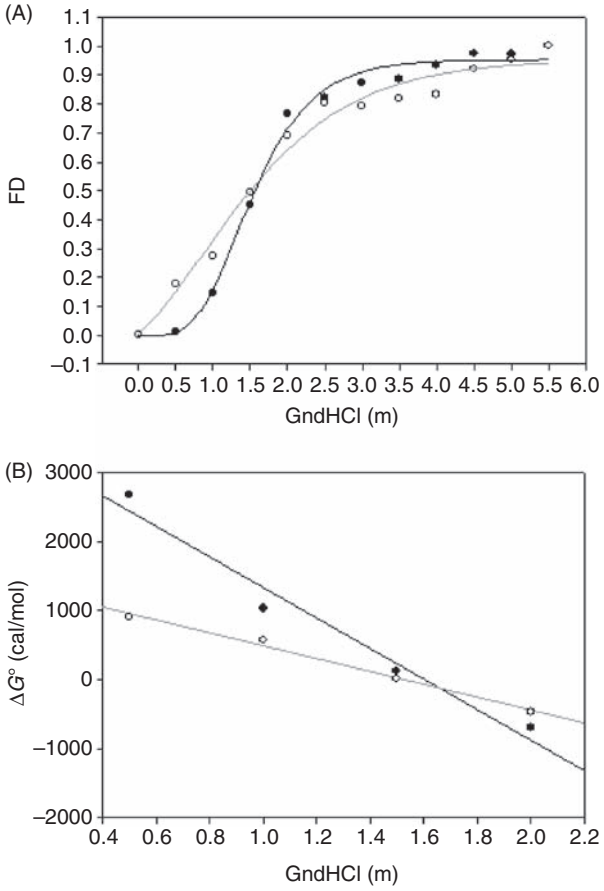


**Fig. 4**. (A) Chemical denaturation of apoAI (filled circles) and apoAI-LPS (open circles) at different GdnHCl concentrations (0–5.5 M) in buffer A at pH 7.4, and 25°C quantified from fluorescence intensity at 333 nm. $f_D$ corresponds to molar fraction of denatured molecules and was estimated as described in Materials and Methods. The excitation wavelength was 295 nm. Data were fitted to sigmoidal curves using the curve-fitting procedures in SigmaPlot (Jandel Scientific, San Rafael, CA, USA). The black and gray lines correspond to apoAI and apoAI–LPS denaturation curves, respectively. The protein concentration was 2.85 μM in both cases. (B) Dependence of the unfolding free energy ($\Delta G^\circ$) with denaturant concentration for apoAI (filled black circles) and apoAI–LPS (filled gray circles). $m$ and $\Delta G^\circ_{H_2O}$ were calculated from the slope and ordinate intercept, respectively.

*Circular dichroism spectroscopy*

Circular dichroism (CD) is a technique sensitive to the chirality of the environment. The far-UV region of proteins absorbance spectrum (190–250 nm) is dominated by the electronic absorbance from peptide bonds and provides information about the secondary structure of a protein because each category of secondary structure (*e.g.* α-helix, β-sheet) has a different effect on the chiral environment of the peptide bond. Far-UV CD spectra recorded for lipid-free apoAI and after its incubation with LPS are characteristic for an α-helix structure with two negative bands at 222 and 208 nm and a positive one at 193 nm as shown in Figure 5; therefore, the presence of LPS does not modify the secondary structure predominant in apoAI. At near-physiological temperatures, the secondary structure of apoAI is characterized by 55% helical content, as inferred from the molar ellipticity at 222 nm, according to the literature.[31,32] The helical content after LPS interaction decreases to 46%. These results suggest that, in the presence of LPS, unfolding of certain α-helix portions occurs in some regions of the protein.

*Cross-linking of $^{125}I$ ASD–LPS to apoAI*

In order to test if a direct interaction between LPS and apoAI takes place, cross-linking procedures using

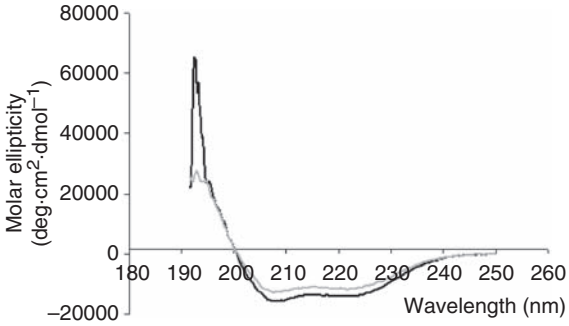


**Fig. 5**. Circular dichroism spectra in the far-UV (190–250 nm) region were collected for apoAI in the absence (black line) or presence (gray line) of LPS. Protein concentration: 100 μg/ml. ApoAI–LPS were used in 1 : 2.8 (molar ratio).

$^{125}$I-ASD–LPS (described in Materials and Methods), including UV irradiation, SDS-PAGE and autoradiography, were done.

The *N*-hydroxysuccinimidyl derivative can easily react with primary amines under the condition applied for the coupling step (0.1 M borate buffer, pH 8.5). Since core and O-polysaccharide glucosamine are both quantitatively acetylated, the more likely site for attachment of this ASD compound is via an amide linkage to the primary ethanolamine. Phosphoethanolamine serves as the major attachment site for the ASD label on LPS.

Incorporation of $^{125}$I into apoAI could be detected as seen in Figure 6, corroborating the direct interaction of LPS with apoAI.

### *Chemical cleavage of apoAI-$^{125}$I ASD–LPS with CNBr*

In order to determine which portion of the protein interacts with LPS, cleavage of apoAI-$^{125}$I ASD–LPS with CNBr was performed. The proteolytic fragments were analyzed by tricine SDS-PAGE and autoradiography yielded the results shown in Figure 7.

Apolipoprotein AI contains three methionine residues at which cleavage with CNBr occurs: residues Met 86, Met 112, and Met 148 and only four polypeptides should be obtained by complete cleavage. However, because of incomplete cleavage, a more complex pattern, of 8 peptide bands (A–H) can be observed (Fig. 7A).

Autoradiography analysis of the proteolytic products obtained by CNBr cleavage (Fig. 7B) shows that five peptides (B, C, E, F and H) are radioactively labeled. A different label radioactivity can be observed in each band, which is possibly due to differences in their affinity to LPS.

As we focus our interest on the minimal portion of apoAI able to bind LPS with high affinity, the N-terminal sequence of fragments E, F and H (Fig. 7B) were obtained. These fragments correspond

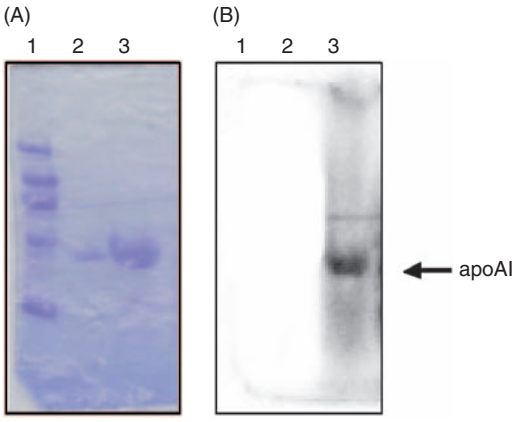


**Fig. 6**. Cross-linking of $^{125}$I-ASD–LPS with apoAI. For cross-linking experiments, $^{125}$I-ASD–LPS (5 μg) incubated with apoAI (1 : 2.8 protein : LPS molar ratio) were subjected to photolysis. Sodium dodecyl sulfate-PAGE electrophoresis was carried out on 4–25% continuous gradient gels (10 μg protein concentration). Proteins were stained with Coomassie Blue (A) and subsequent autoradiography was performed on Storm 840 (B). Lane 1, molecular mass markers; lane 2, apoAI standard; lane 3, apoAI-$^{125}$I-ASD–LPS interaction.

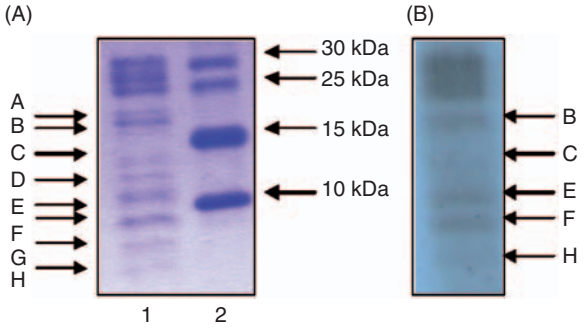


**Fig. 7**. Chemical cleavage of apoAI-$^{125}$I-ASD–LPS with CNBr. Apo AI-$^{125}$I-ASD–LPS cleavage with CNBr was analyzed by tricine SDS-PAGE. The proteolytic fragments were stained with Coomasie Blue (A) and exposed to X-Omat film (Kodak) for radioactive detection (B). The arrows indicate the proteolytic fragments. Panel A: lane 1, CNBr proteolytic fragments of apoAI-$^{125}$I-ASD-LPS, lane 2, MWM (Pharmacia).

to segments from residues 113–148 (fragment E), 149–243 (fragment F) and 1–112 (fragment H).

However, because fragment F which correspond to the C-terminal half of apoAI contains a higher label of radioactivity, we chose this fragment to test the capability of endotoxin neutralization by measurement of TNF-α release.

### *Tumor necrosis factor-α release measurements*

Tumor necrosis factor-α is one of the major cytokines that is synthesized and secreted by macrophages upon stimulation by LPS. The effect of apoAI and fragment F on LPS induced TNF-α release was monitored by ELISA. For these studies, fragment F was purified by electroelution as described in Materials and Methods.

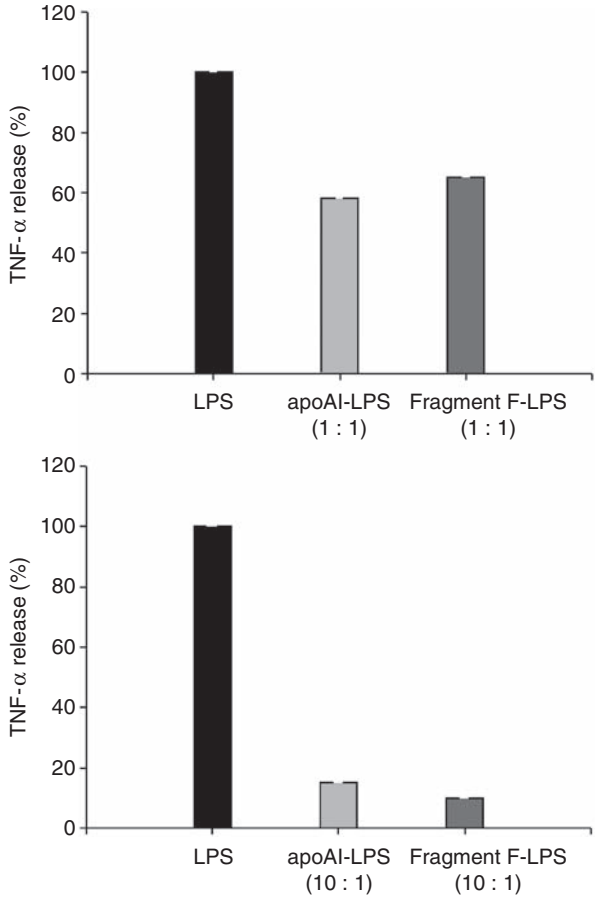


**Fig. 8**. Tumor necrosis factor-α release (%) by RAW 264.7 cells after incubation with LPS (10 ng/ml) (black bar) apoAI : LPS mixture (light gray bar) and fragment F : LPS mixture (dark gray bar) at 1 : 1 w/w ratio (A) and LPS (black bar) (10 ng/ml) and apoAI : LPS mixture (light gray bar) and fragment F : LPS mixture (dark gray bar) at 1 : 1o w/w ratio (B). Each experiment was done least three times, and the data were averaged.

Stimulation of cells with LPS resulted in TNF-α production, taken as 100%. Pre-incubation of LPS (10 ng/ml) with both apoAI and fragment F, in two different concentrations (protein/fragment F : LPS; 1 : 1 and 10 : 1, w/w), resulted in a reduction in the level of TNF-α release by the cells (Fig. 8). A 58% and 15% TNF-α release were observed in the presence of 1 : 1 w/w and 10 : 1 w/w apoAI : LPS, respectively. In addition, 65% and 10% of TNF-α release were obtained when the fragment F was assayed at of 1 : 1 w/w and 10 : 1 w/w apoAI : LPS, respectively. The respective control with apoAI and fragment F were done and subtracted in each experiment.

## DISCUSSION

Structural analysis of peptides that naturally bind LPS can be helpful in identifying those molecular features involved in binding to, and neutralizing, LPS. Regardless of the molecular structure of a given peptide, the underlying theme for efficient interaction with, and binding to, LPS is known from many studies to be a net positive charge and high hydrophobicity, usually in the context of an amphipathic structure. Positively charged residues from the peptide presumably promote interaction with negatively charged groups on LPS, that is, phosphates on the lipid A glucosamines and/or those in the inner core polysaccharide unit; while hydrophobic residues from the peptide interact with acyl chains on lipid A.

Mature human apoAI contains 243 amino acid residues[33] with 11-mer and 22-mer homologous repeats that are predicted to form amphipathic α-helices that interact with lipids through their hydrophobic face. The helices are linked by short and flexible β-turns usually containing a proline residue. Lipid-free apoAI is thought to be a bundle of helices.[34]

A high conformational flexibility in apoAI is needed for its existence in different states – lipid-free, lipid-poor, and discoidal or spherical lipoproteins of different size. The conformational flexibility of apoAI could also play a role in the interaction with LPS, in both lipid-free and also in lipid-associated states.

Although there are no changes in the $\lambda_{max}$ of Trp spectra of lipid-free apoAI after its interaction with LPS, a decrease in the intrinsic fluorescence intensity is observed (Fig. 1). This is due to a more relaxed structure of apoAI–LPS complex, as suggested by the denaturation behavior, with a higher water accessibility and also by the presence of polar groups of the associated LPS.

The denaturation curves give important information concerning protein stability in the free or LPS-associated state. As seen in Figure 4, the interaction of LPS with apoAI is responsible of a decreased co-operativity of the unfolding process. As is known, molten globule proteins typically unfold at low concentrations of denaturant and do not show a sigmoidal unfolding curve. As a consequence of the interaction of apoAI with LPS, the protein is less stable, as was demonstrated by a lower $\Delta G^{\circ}_{H_2O}$ value. $\Delta G^{\circ}$ decreases more slowly with increasing denaturant concentration in the presence of LPS in comparison with lipid-free apoAI, as was expected, due to the lower hydrophobic surface exposed during denaturation. This is due to a more relaxed structure of apoAI–LPS complex and also because the presence of polar groups of the associated LPS. These facts are also reflected in lower $m$ values in comparison with free apoAI.

Apolipoprotein AI has been proposed to unfold and bind lipids via a molten globule state.[35] In our study, we also found that apoAI–LPS complex presents a molten globule-like behavior.

Experiments of Trp oxidation with NBS render the same result independently, if the protein is in buffer or if it was previously incubated with LPS. As a first approach, it is possible to speculate that the N-terminal half of the protein, where 3 of the 4 Trp amino-acid residues are located, are not involved in the interaction with LPS.

The cross-linking assay between apoAI and $^{125}$I-ASD–LPS (Fig. 6) followed by chemical cleavage with CNBr, gave a series of fragments which were analyzed by tricine SDS-PAGE and autoradiography (Fig. 7). These fragments were electroeluted and sequenced by the Edman method, showing that the fragment containing the higher level of radioactivity corresponds to N-terminal sequence RDRARA. According to the molecular mass and the N-terminal sequence, the fragment named 'F', corresponds to the C-terminal half of apoAI (residues 148–243). Together, our results confirm the hypothesis that the C-terminal half of apo-AI is involved in the binding with LPS. For this reason, we chose the fragment F of apoAI to test the capability of neutralize endotoxic effect of LPS by TNF-α release measurements. Pre-incubation of LPS (10 ng/ml) with the C-terminal half of apoAI resulted in a reduction of the TNF-α release by the cells in 90% in comparison with the 85% observed for the LPS incubated with free apoAI (Fig. 8). This result confirms the important role of the C-terminal half of apoAI in the binding and neutralization of the endotoxic effect of LPS.

The N-terminal half of apoAI (approximately amino-acids 1–139) is highly α-helical and primarily responsible for the stability of the protein in solution, while the C-terminal half (approximately amino-acids 140–243) is relatively unstable. Roberts *et al*.[36] studied limited proteolysis of lipid-free apoAI, and they found that the C-terminal half (in their case, approximately amino-acids 190–243) of lipid-free apoAI is highly susceptible to proteolysis, whereas the N-terminus is less exposed. From analysis of the cleavage patterns generated, a model of lipid-free apoAI, consisting of a bundle of α-helices in the N-terminal region with an unorganized C-terminus was constructed.

Details of the conformation and lipid interaction of a C-terminal 46-residue peptide, $^{(198–243)}$apoAI, encompassing putative helix repeats 10 and 9 and the second half of repeat 8 from the C-terminus of apoAI was published by Zhu and Atkinson.[37] Far-UV circular dichroism spectra showed that $^{(198–243)}$apoAI is also unfolded in aqueous solution. They showed direct evidence that the C-terminal peptide model can mimic the interaction with the phospholipid of plasma apoAI to form two sizes of homogeneous discoidal complexes.

A synthetic peptide containing amino-acids 220–241 of apoAI has been shown to have the highest affinity toward lipids among the other apoAI helices. Supporting evidence for the existence of α-helical structure in repeat 10 comes from the work of Palgunachari *et al*., who showed that, among a series of synthetic peptides corresponding to the helical repeats of apoAI, the peptide encompassing residues 220–242 had the highest α-helix content in solution, stability and lipid binding potential of all the peptides studied.[38]

Segrest and colleagues[39] proposed that the α-helices of apolipoproteins are not all equivalent in their affinities toward lipids. The differences in affinity do not appear to be only related to their hydrophobic moment but also to the distribution of charged residues along the axis of the helix. Amphipathic helices are classified into seven major and distinct classes (A, H, L, G, K, C, and M) based upon a detailed analysis of their physicochemical and structural properties. The most frequent helix class found in exchangeable apolipoproteins is class A, which is characterized by a unique clustering of positively charged amino acid residues at the polar–non-polar interface and negatively charged residues at the center of the polar face. Six class A helices have been identified in apoAI,[40,41] three of which are in the N-terminal half of apoAI (helices 44–65, 66–87, 121–142), and the other three are in the C-terminal half (helices 143–164, 166–186, and 187–208). In addition, two other helix types were also identified: class G* (helix 8–33) and class Y (helices 88–98, 99–120 in the N-terminal half of apoAI and 209–219, and 220–241 in the C-terminal half of apoAI). The basic feature of the class Y motif are two negative residue clusters on the polar face separating the two arms and the base of the Y motif formed by three positive residue clusters. It was proposed that the lipid affinity correlates with the extent to which a helix domain fits to class A motif.[40,42]

Experiments using the hydrophobic reagent 3-(trifluoromethyl)-3-(*m*-[$^{125}$I]-iodophenyl-diazirine, demonstrated the apoAI regions in contact with the lipid phase in the rHDL discs. Two protein regions loosely bound to lipids in HDL were detected – a C-terminal domain and a central one located between residues 87 and 112. They consist of class Y amphipathic α-helices.

While important functions have been attributed to the C-terminal region of apoAI in initial binding to lipid[43] and interaction with cells,[44] little is known about its involvement in LPS interaction. Our results show that lipid-free apoAI can directly interact with LPS, and the helical stretches along the protein are responsible for the multiple regions able to interact with LPS, as seen in Figure 7B, by the multiple fragments radiolabeled after photochemical cross-linking.

According to our previous results about the partition of LPS in lipid membranes (Henning *et al*., unpublished results), we suggest that, when the protein is associated with lipid such as in HDL particles, partition of LPS in the lipid matrix of the lipoprotein could favor the

interaction between the lipid-binding domain of apoAI, which is exposed to the lipid matrix of HDL, and LPS.

On the other hand, according to Corsico *et al*.,[45] the C-terminal half of the protein presents a loose region capable of binding membrane lipids, and taking into account that this region is the one that we found to interact with LPS, we can speculate that the same region involved in the interaction with lipids is involved in the interaction with LPS.

## Conclusions

The C-terminal half of apoAI may be involved in LPS interaction in both lipid-free conditions or when the protein is associated with lipid in HDL. The results of this research suggest that the C-terminal half of apoAI presents beneficial anti-inflammatory effects. Peptides derived from this part of apoAI molecule have great potential as a therapeutic agent in inflammatory diseases.

## Acknowledgements

This work was supported by grants from the Comisión de Investigaciones Científicas de la Provincia de Buenos Aires CIC-PBA. Argentina and Agencia de Promoción Científica y Tecnológica ANPCyT, Argentina. MFH is a fellow of Consejo de Investigaciones Científicas y Tecnológicas CONICET, Argentina. VH is a member of the Carrera del Investigador of Consejo de Investigaciones Científicas y Tecnológicas CONICET, Argentina. LSB is a member of the Carrera del Investigador Comisión de Investigaciones Científicas de la Provincia de Buenos Aires, Argentina.

## References

1. Wu A, Hinds CJ, Thiemermann C. High-density lipoproteins in sepsis and septic shock: metabolism, actions, and therapeutic applications. *Shock* 2004; **21**: 210–221.
2. van Leeuwen HJ, Heezius EC, Dallinga GM *et al*. Lipoprotein metabolism in patients with severe sepsis. *Crit Care Med* 2003; **31**: 1359–1366.
3. Liao XL, Ma J, Lou B *et al*. Alteration of the components in serum high density lipoprotein during the acute phase reaction induced by lipopolysaccharide. *Fudan Univ J Med Sci* 2004; **31**: 469–472.
4. Van Lenten BJ, Hama SY, de Beer FC *et al*. Anti-inflammatory HDL becomes pro-inflammatory during the acute phase response. Loss of protective effect of HDL against LDL oxidation in aortic wall cell cocultures. *J Clin Invest* 1995; **96**: 2758–2767.
5. Parker TS, Levine DM, Chang JC *et al*. Reconstituted high-density lipoprotein neutralizes Gram-negative bacterial lipopolysaccharides in human whole blood. *Infect Immun* 1995; **63**: 253–258.
6. Gordon BR, Parker TS, Levine DM *et al*. Low lipid concentrations in critical illness: implications for preventing and treating endotoxemia. *Crit Care Med* 1996; **24**: 584–589.
7. Massamiri T, Tobias PS, Curtiss LK. Structural determinants for the interaction of lipopolysaccharide binding protein with purified high density lipoproteins: role of apolipoprotein A-I. *J Lipid Res* 1997; **38**: 516–525.
8. Park CT, Wright SD. Plasma lipopolysaccharide-binding protein is found associated with a particle containing apolipoprotein A-I, phospholipid, and factor H-related proteins. *J Biol Chem* 1996; **271**: 18054–18060.
9. Emancipator K, Csako G, Elin RJ. *In vitro* inactivation of bacterial endotoxin by human lipoproteins and apolipoproteins. *Infect Immun* 1992; **60**: 596–601.
10. Yan Y, Li Y, Lou B *et al*. Beneficial effects of ApoA-I on LPS-induced acute lung injury and endotoxemia in mice. *Life Sci* 2006; **79**: 210–215.
11. Ma XL, Liao B, Wu MP. Role of apolipoprotein A-I in protecting against endotoxin toxicity. *Acta Biochim Biophys Sinica* 2004; **36**: 419–424.
12. Tricerri A, Corsico B, Toledo JD *et al*. Conformation of apolipoprotein AI in reconstituted lipoprotein particles and particle-membrane interaction: effect of cholesterol. *Biochim Biophys Acta* 1998; **1391**: 67–78.
13. Aurell C, Wistrom A. Critical aggregation concentrations of Gram-negative bacterial lipopolysaccharides (LPS). *Biochem Biophys Res Commun* 1998; **253**: 119–123.
14. Valpuesta J, Goñi F, Macarulla J. Tryptophan fluorescence of mitochondrial complex III reconstituted in phosphatidylcholine bilayers. *Arch Biochem Biophys* 1987; **257**: 285–292.
15. Ohnishi M, Kawagishi T. Stopped-flow studies on the chemical modification with *N*-bromosuccinimide of model compounds of tryptophan residues. *J Biochem* 1980; **87**: 273–279.
16. Stryer L. The interaction of a naphthalene dye with apomyoglobin and apohemoglobin. A fluorescent probe of nonpolar binding sites. *J Mol Biol* 1965; **13**: 482–495.
17. Lackowicz J. *Principles of Fluorescence Spectroscopy*. New York: Plenum, 1984.
18. Schmid F. Spectral methods of characterizing protein conformation and conformational changes. In: Creighton TE. (ed) *Protein Structure: A Practical Approach*. Oxford: IRL, 1989. p 251.
19. Chen Y, Yang J, Martinez H. Determination of the secondary structures of proteins by circular dichroism and optical rotary dispersion. *Biochemistry* 1972; **11**: 4120–4131.
20. Wollenweber HW, Morrison DC. Synthesis and biochemical characterization of a photoactivatable, iodinatable, cleavable bacterial lipopolysaccharide derivative. *J Biol Chem* 1985; **260**: 15068–15074.
21. Ulevitch RJ. The preparation and characterization of a radioiodinated bacterial lipopolysaccharide. *Immunochemistry* 1978; **15**: 157–164.
22. Karkhanis Y, Zeltner J, Jackson J *et al*. A new and improved microassay to determine 2-keto-3-deoxyoctonate in lipopolysaccharide of Gram-negative bacteria. *Anal Biochem* 1978; **85**: 595–601.
23. Laemmli U. Cleavage of structural proteins during the assembly of the head of bacteriophage T4. *Nature* 1970; **227**: 680–685.
24. Schägger H, von Jagow G. Tricine-sodium dodecyl sulfate-polyacrylamide gel electrophoresis for the separation of proteins in the range from 1 to 100 kDa. *Anal Biochem* 1987; **166**: 368–379.
25. Hager D, Burgess R. Elution of proteins from sodium dodecyl sulfate-polyacrylamide gels, removal of sodium dodecyl sulfate, and renaturation of enzymatic activity: results with sigma subunit of *Escherichia coli* RNA polymerase, wheat germ DNA topoisomerase, and other enzymes. *Anal Biochem* 1980; **109**: 76–86.
26. Ohhashi T, Moritani C, Andoh H *et al*. Preparative high-yield electroelution of proteins after separation by sodium dodecyl

sulphate-polyacrylamide gel electrophoresis and its application to analysis of amino acid sequences and to raise antibodies. *J Chromatogr* 1991; **585**: 153–159.
27. Lowry O, Rosebrough N, Farr A *et al*. Protein measurement with the Folin phenol reagent. *J Biol Chem* 1951; **193**: 265–275.
28. Burstein EA, Vedenkina NS, Ivkova MN. Fluorescence and the location of tryptophan residues in protein molecules. *Photochem Photobiol* 1973; **18**: 263–279.
29. Pace C. Determination and analysis of urea and guanidine hydrochloride denaturation curves. *Methods Enzymol* 1986; **131**: 266–280.
30. Myers J, Pace C, Scholtz J. Denaturant m values and heat capacity changes: relation to changes in accessible surface areas of protein unfolding. *Protein Sci* 1995; **4**: 2138–2148.
31. Atkinson D, Small DM. Recombinant lipoproteins: implications for structure and assembly of native lipoproteins. *Annu Rev Biophys Biophys Chem* 1986; **15**: 403–456.
32. Dalton M, Swaney J. Structural and functional domains of apolipoprotein AI within high density lipoproteins. *J Biol Chem* 1993; **268**: 19274–19283.
33. Brewer Jr HB, Fairwell T, LaRue A *et al*. The amino acid sequence of human APOA-I, an apolipoprotein isolated from high density lipoproteins. *Biochem Biophys Res Commun* 1978; **80**: 623–630.
34. Davidson WS, Arnvig-McGuire K, Kennedy A *et al*. Structural organization of the N-terminal domain of apolipoprotein A–I: studies of tryptophan mutants. *Biochemistry* 1999; **38**: 14387–14395.
35. Gursky O, Atkinson D. Thermal unfolding of human high-density apolipoprotein A-1: implications for a lipid-free molten globular state. *Proc Natl Acad Sci USA* 1996; **93**: 2991–1995.
36. Roberts LM, Ray MJ, Shih TW *et al*. Structural analysis of apolipoprotein A–I: limited proteolysis of methionine-reduced and -oxidized lipid-free and lipid-bound human Apo A-I. *Biochemistry* 1997; **36**: 7615–7624.
37. Zhu H, Atkinson D. Conformation and lipid binding of a C-terminal 198–243. peptide of human apolipoprotein A-I. *Biochemistry* 2007; **46**: 1624–1634.
38. Palgunachari M, Mishra V, Lund-Katz S *et al*. Only the two end helixes of eight tandem amphipathic helical domains of human apoAI have significant lipid affinity. Implications for HDL assembly. *Arterioscler Thromb Vasc Biol* 1996; **16**: 328–338.
39. Segrest J, Garber D, Brouillette C *et al*. The amphipathic alpha helix: a multifunctional structural motif in plasma apolipoproteins. *Adv Protein Chem* 1994; **45**: 303–369.
40. Segrest JP, Jones MK, De Loof H *et al*. The amphipathic helix in the exchangeable apolipoproteins: a review of secondary structure and function. *J Lipid Res* 1992; **33**: 141–166.
41. Frank P, Marcel Y. Apolipoprotein AI: structure–function relationship. *J Lipid Res* 2000; **41**: 853–872.
42. Segrest J, De Loof H, Dohlman J *et al*. Amphipathic helix motif: classes and properties. *Proteins* 1990; **8**: 103–117.
43. Ji Y, Jonas A. Properties of an N-terminal proteolytic fragment of apolipoprotein AI in solution and in reconstituted high density lipoproteins. *J Biol Chem* 1995; **270**: 11290–11297.
44. Morrison J, Fidge N, Tozuka M. Determination of the structural domain of apoAI recognized by high density lipoprotein receptors. *J Biol Chem* 1991; **266**: 18780–18785.
45. Córsico B, Toledo J, Garda H. Evidence for a central apolipoprotein AI domain loosely bound to lipids in discoidal lipoproteins that is capable of penetrating the bilayer of phospholipid vesicles. *J Biol Chem* 2001; **276**: 16978–16985.